D. A. Anderson, "Disc and Ring Exciter Shape Effects on Flat-Panel Loudspeakers," *J. Audio Eng. Soc.*, vol. 73, no. 1/2, pp. 75–81 (2025 Jan./Feb.). https://doi.org/10.17743/jaes.2022.0187.

Disc and Ring Exciter Shape Effects on Flat-Panel Loudspeakers

DAVID A. ANDERSON,* *AES Associate Member*
(and10445@d.umn.edu)

Department of Electrical Engineering, University of Minnesota Duluth, Duluth, MN, USA

Flat-panel loudspeaker exciters are moving coil motors with a coupling surface, often shaped like a ring or disc, that attaches to the surface of a plate. Simulations normally treat the exciter as acting like a point force, but in reality, the ring or disc shape can have a significant influence on the frequency response of the plate at middle and high frequencies. Equations to model the effects of disc and ring shapes are introduced, and simulations demonstrate that these exciter coupling shapes impose a low-pass filtering effect with sharp nodes in the frequency response of the vibrating surface, with rings having a lower cutoff frequency than discs. Comparisons between simulation and experimental data are provided.

0 INTRODUCTION

Flat-panel loudspeakers, also referred to as distributed mode loudspeakers [1] or bending wave loudspeakers [2], are flat plates of essentially any shape excited into bending motion by one or more vibration-inducing "exciters" that use overlapping resonant modes to efficiently radiate sound [3]. Exciters, which are often made using voice coil motors or piezoelectric bending patches, are used to create speakers from display screens [4] and hermetically sealed cases and are also popular among hobbyists looking to make speakers from a wide variety of plate materials.

This paper specifically concerns voice coil exciters, which are commercially available and easy to set up and use for both manufacturers and hobbyists. Roberts [5] developed a model for the simulation and design of exciters based on the bulk behavior of panel motion that assumes no modal behavior, and the author of this paper developed a somewhat more complex model that incorporates modal behavior [6]. Both models are limited in utility at high frequencies because they were "derived for a point contact," but practical exciters "[drive] the panel at the periphery of the voice coil."[5]

Exciter manufacturers have been offering larger and heavier exciters in recent years, with wider voice coils meant for high-power handling capabilities [7], so the effects from the ring or disc coupling shape will be more prominent. The ring-shaped adhesive coupling surface that attaches the exciter to the plate is therefore larger, and its effects are therefore seen at lower frequencies. Additionally, new exciter designs are also incorporating flat disc-shaped coupling surfaces [7]. Fig. 1 shows a picture of two commercially-available exciter models (one ring and one disc), that are used in the experiments in SEC. 3.

In this paper, the assumption that waves on the plate surface are sinusoidal in shape can be used to derive some simple equations for how the ring and disc shapes influence the vibrational and acoustic response of a plate when compared with the simpler, theoretical point source exciter element. The first section derives equations that relate disc or ring dimensions to panel wavelength and defines cutoff frequencies for a given exciter shape and material. The second section shows numerical simulation results for a selection of panel shapes and exciter shapes, comparing results with the formulas derived in the first section and making use of a simulation model developed in [6]. The third section gives experimental results and compares them with simulations. The final section gives conclusions and suggestions for further work.

1 BACKGROUND

The vibrational excursion $Z(x, y, t, f_E(x, y))$ of strings, beams, membranes, and plates in response to an excitation force profile $f_E(x, y)$ can be represented using the following equation [8, 9]:

$$Z(x, y, t, f_E(x, y)) = \sum_{k'} \alpha(k', f_E(x, y)) G(x, y, k') P(k', j\omega t). \quad (1)$$

*To whom correspondence should be addressed, email: and10445@d.umn.edu

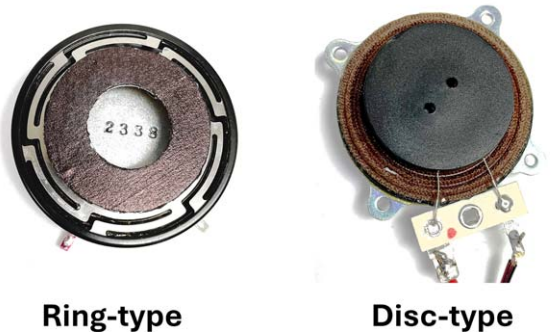

Fig. 1. A ring-type exciter (DAEX32EP-4) and a disc-type exciter (EX30HESF2-4) obtained from [7].

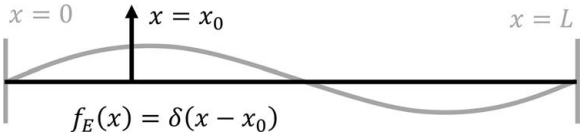

Fig. 2. A diagram of a 1D vibrating structure (gray) and a point source excitation profile (black).

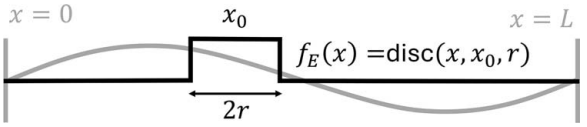

Fig. 3. A diagram of a 1D vibrating structure (gray) and a disc-type excitation profile (black).

The function $G(x, y, k')$ represents a spatial mode shape with x and y representing spatial position (for strings or beams the y-dimension is removed) and k' being a modal index variable that is proportional to wavenumber. $P(k', j\omega t)$ is the frequency response of the mode defined by k', governed by the vibroelastic behavior of the structure, generally represented by a single resonant frequency with quality factor Q, although a more complicated response is possible [6]. The function $\alpha(k', f_E(x, y))$ represents the "coupling" between the mode shape defined by k' and the excitation force spatial profile $f_E(x, y)$, and can be calculated as

$$\alpha(k', f_E(x, y)) = \int_S G(x, y, k') f_E(x, y) dS, \tag{2}$$

where S is the total surface of the vibrating shape.

Assuming Cartesian coordinates (polar coordinates may instead be necessary if analyzing the behavior of circular plates), spatial mode functions may be broken into separate x and y domain functions as $G(x, y, k') = \theta(x, k')\phi(y, k')$. The functions θ and ϕ often take sinusoidal shapes, especially with "freely-supported" or "simply-supported" boundary edge conditions, but may include additional hyperbolic sinusoidal shapes under free or fixed boundary conditions. These hyperbolic sinusoidal shapes, however, become insignificant at short wavelengths relative to the plate dimensions [8], so for the sake of simplicity, only sinusoidal mode functions will be assumed.

The excitation force spatial profile for a point force is $f_E(x, y) = \delta(x - x_0, y - y_0)$, where x_0 and y_0 are the location of the exciter and δ represents the Dirac delta function [10]. For a disc-shaped exciter centered at (x_0, y_0) and with radius r, the excitation force function can be written as

$$f_E(x, y) = \frac{1}{\pi r^2} \begin{cases} 1 & (x - x_0)^2 + (y - y_0)^2 \leq r^2 \\ 0 & \text{otherwise} \end{cases}, \tag{3}$$

which will be referred to as $\frac{1}{\pi r^2}\text{disc}(x, y, x_0, y_0, r)$ for brevity. Finally, the excitation function for a ring-shaped exciter with outer radius r_O and inner radius r_I centered at (x_0, y_0) is then

$$f_E(x, y) = \frac{\text{disc}(x, y, x_0, y_0, r_O) - \text{disc}(x, y, x_0, y_0, r_I)}{\pi(r_O^2 - r_I^2)}. \tag{4}$$

Unfortunately, gaining insights by plugging f_E functions into Eq. (2) is only analytically straightforward for the case of the point source. Instead, it is more straightforward to analyze excitation shape behavior in 1D structures and extrapolate the results to 2D structures through the relationship to bending wavelengths, which will be done in the following sections.

1.1 1D Analysis

Assuming a 1D structure of length L, k' is simply equal to wavenumber k, and mode shape functions will take the simple form $\theta(x, k) = \sin(kx)$; the coupling factor can be evaluated as

$$\alpha(k, f_E(x)) = \int_0^L \sin(kx) f_E(x) dx, \tag{5}$$

which can be considered the Fourier sine transform in k-space evaluated over a small spatial region for the excitation function. These expressions can be evaluated using transform pairs but will be more explicitly calculated here so that the relationship to physical quantities is more obvious.

For a point source excitation function, as seen in Fig. 2, the coupling factor from Eq. (5) works out to $\alpha(k, \delta(x - x_0)) = \sin(kx_0)$. However, this function depends on x_0, the location of the exciter. Because the difference between exciter shapes is of more interest than the response at any one exciter position, the RMS value over all spatial positions will be used, which for the point source exciter is

$$\sqrt{\frac{1}{L}\int_0^L \sin^2(kx_0) dx_0} = \frac{1}{\sqrt{2}}. \tag{6}$$

The result is a constant value with no dependence on wavenumber k, which tells the reader that all wavelengths are excited equally by a point source excitation function.

1.1.1 1D Disc

The 1D excitation function for a disc-shaped driver (now just a rectangle, visualized in Fig. 3) centered at x_0 with radius r is

$$f_E(x) = \frac{1}{2r} \begin{cases} 1 & x_0 - r \leq x \leq x_0 + r \\ 0 & \text{otherwise} \end{cases}, \tag{7}$$

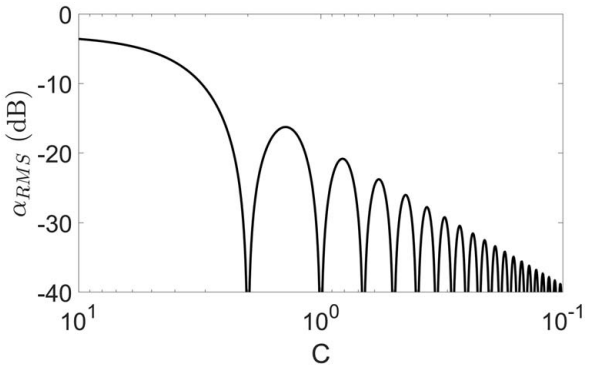

Fig. 4. A graph of α_{RMS} for a disc as a function of C, which is defined as λ/r.

which will be simplified as disc(x, x_0, r) for brevity. Inserting Eq. (7) into Eq. (5), the coupling factor equation then becomes

$$\alpha(k, \text{disc}(x, x_0, r)) = \frac{1}{2r}\int_{x_0-r}^{x_0+r} \sin(kx)dx \tag{8}$$

$$= \frac{-1}{rk}\sin(rk)\sin(kx_0), \tag{9}$$

and the RMS value over all x_0 locations works out to $\left|\frac{1}{\sqrt{2}rk}\sin(rk)\right|$, which can be simplified as $\left|\frac{1}{\sqrt{2}}\text{sinc}(rk)\right|$.

Wavenumber k is then equal to $\frac{2\pi}{\lambda} = \frac{m\pi}{L}$, where λ is the wavelength and $m = 1, 2, 3, \ldots$ to represent mode shape index (the number of half-wavelengths on the 1D surface). Defining a new variable, $C = \frac{\lambda}{r}$, the RMS coupling factor is

$$\alpha_{RMS} = \left|\frac{C}{2\sqrt{2}\pi}\sin\left(\frac{2\pi}{C}\right)\right|, \tag{10}$$

which can be simplified further as an absolute value sinc function,

$$\alpha_{RMS} = \left|\frac{1}{\sqrt{2}}\text{sinc}\left(\frac{2\pi}{C}\right)\right|. \tag{11}$$

When the wavelength is much greater than the radius of the exciter, C approaches infinity and sinc $\left(\frac{2\pi}{C}\right)$ will approach 1. In this case, the coupling factor equation becomes identical to that for a point source exciter from Eq. (6).

Fig. 4 plots α_{RMS} vs. C from Eq. (10). It can be seen that the disc shape introduces a low-pass–filtering effect that has an initial null at $C = 2$ (where the wavelength is equal to the diameter of the exciter) and an initial -3 dB point at $C \approx 4.54$. This result means that the effective bandwidth of a disc exciter (where it acts like a point force exciter) extends from $C = 4.54$ to $C = \infty$.

These equations assume that the disc is perfectly rigid (does not bend or exhibit its own resonances) and that, although it applies force evenly to the plate surface, the plate is still free to bend around the shape of the disc. The second assumption is realistic because exciters are usually bonded to the plate with adhesive foam tape such that the plate can still bend at that area. The first assumption will depend largely on the disc materials and will be explored further in SEC. 3 on Experimental Validation.

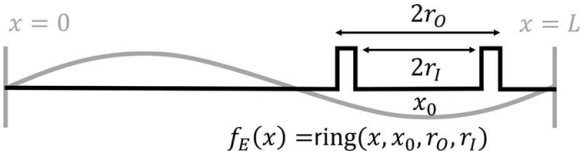

Fig. 5. A diagram of a 1D vibrating structure (gray) and a ring-type excitation profile (black).

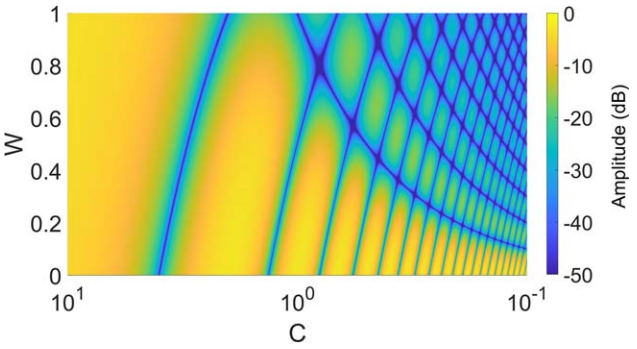

Fig. 6. A graph of α_{RMS} from Eq. (15) for a ring as a function of C and W. $W = 1$ is a disc (matching Fig. 4), and $W = 0$ is a thin ring.

1.1.2 1D Ring

The 1D excitation function for a ring-shaped driver (now just two rectangles in 1 dimension, visualized in Fig. 5) centered at x_0 with outer radius r_O and inner radius r_I is

$$f_E(x) = \frac{1}{2(r_O - r_I)}\begin{cases}1 & x_0 - r_O \le x \le x_0 - r_I \\ 1 & x_0 + r_I \le x \le x_0 + r_O \\ 0 & \text{otherwise}\end{cases}, \tag{12}$$

which will be simplified as *ring*(x, x_0, r_O, r_I) for brevity. Inserting Eq. (12) into Eq. (5), the coupling factor equation then becomes

$$\alpha(k, ring(x, x_0, r_O, r_I)) = \frac{1}{2(r_O - r_I)}\left(\int_{x_0-r_O}^{x_0+r_O}\sin(kx)dx - \int_{x_0-r_I}^{x_0+r_I}\sin(kx)dx\right) \tag{13}$$

$$= \left|\frac{1}{\sqrt{2}\pi(r_O - r_I)k}\sin\left(\frac{\pi(r_O - r_I)k}{2}\right)\cos\left(\frac{\pi(r_O + r_I)k}{2}\right)\right|, \tag{14}$$

and, using the simplifications $C = \frac{\lambda}{r_O}$ and $W = \frac{r_O - r_I}{r_O}$,

$$\alpha_{RMS}(k, ring(x, x_0, r_O, r_I)) = \left|\frac{C}{\sqrt{2}\pi W}\sin\left(\frac{\pi W}{C}\right)\cos\left(\frac{\pi(2 - W)}{C}\right)\right|. \tag{15}$$

Fig. 6 shows a surface plot for α_{RMS} vs. C and W. It can be seen that for the thinnest possible ring (when $r_O = r_I$), the first null appears at a higher C value than it would for a disc, specifically at $C = 4$, or when the wavelength is twice the diameter of the ring. The frequency where the

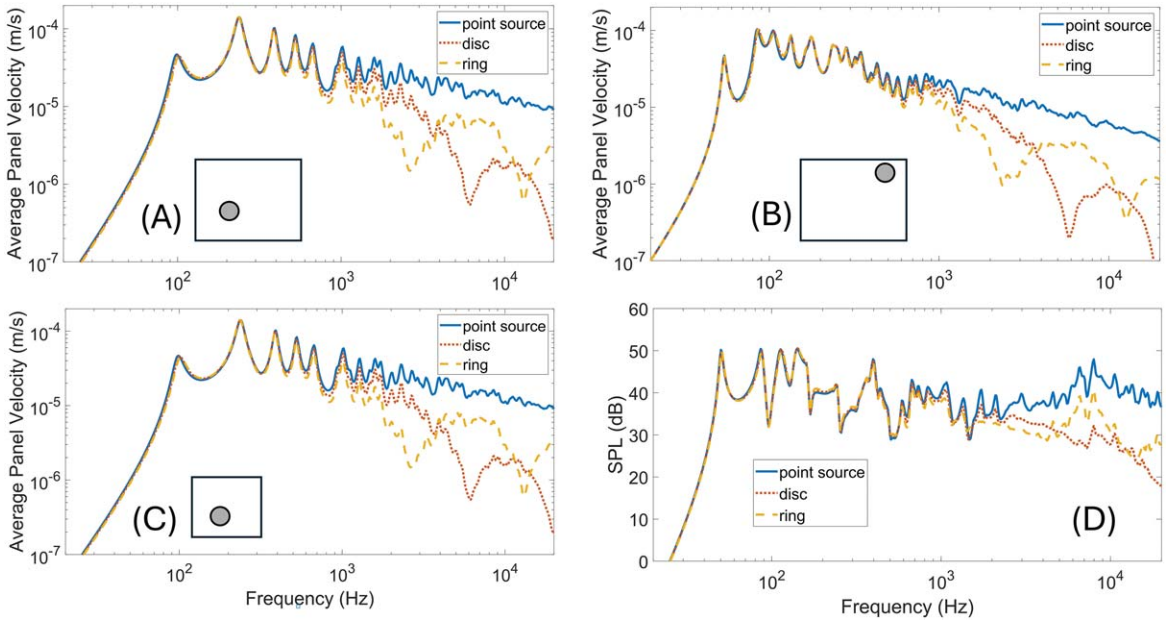

Fig. 7. Graphs of average acrylic plate behavior when driven by an exciter whose shape is either a point, a disc, or a ring. (a) Large acrylic panel with excitation point slightly off-center. (b) Large acrylic panel with excitation source close to the plate corner. (c) Small acrylic panel with excitation point slightly off-center. (d) Average horizon-level acoustic response for each excitation profile matching the graphs from (a). More numeric details for each setup are given in the text.

magnitude drops by 3 dB (subsequently referred to as the cutoff frequency) for a thin ring is at roughly $C = 8.02$, and this metric becomes lower as W increases (the inner radius grows smaller) until it becomes a disc.

1.2 Plate and Beam Wavelengths

The relationship between wavelength λ and frequency f for a thin beam or plate is [9]

$$\lambda = \frac{\sqrt{2\pi}\left(\frac{D}{\rho h}\right)^{\frac{1}{4}}}{\sqrt{f}}, \tag{16}$$

where $D = \frac{Eh^3}{12(1-\nu^2)}$ and it is referred to as the "bending stiffness" of the beam or plate. E is the Young's modulus of the material, h is the thickness of the beam or plate, and ν is the Poisson's ratio of the material. This equation can be used to determine the relationship between cutoff frequency, exciter radius, and bending stiffness. For a disc, as defined above, the cutoff frequency is $C = 4.54$, that when inserted into Eq. (17) works out to

$$4.54 = \frac{\sqrt{2\pi}\left(\frac{D}{\rho h}\right)^{\frac{1}{4}}}{r\sqrt{f}}, \tag{17}$$

so that the cutoff frequency is then

$$f = \frac{2\pi\left(\frac{D}{\rho h}\right)^{\frac{1}{2}}}{4.54r^2}. \tag{18}$$

Similarly, for a thin ring, the cutoff frequency is

$$f = \frac{2\pi\left(\frac{D}{\rho h}\right)^{\frac{1}{2}}}{8.02r^2}. \tag{19}$$

For a plate, these equations assume that the radius of the disc exciter shape and the ring exciter shape is the same for all wavelength directionalities because the wavelength can be oriented completely in the x direction, completely in the y direction, or in a combination of either. As long as the exciter is circular, this condition is true.

2 SIMULATION RESULTS

Simulations presented in this section use the model from [6] and a numerically evaluated disc or ring coupling element to evaluate the efficacy of the equations presented in SEC. 2. The first subsection will explore simulated plate velocity in response to the exciters, and the second subsection will present corresponding results for acoustic radiation from the plates. All results are shown in Fig. 7.

2.1 Mechanical Response

Fig. 7(a) shows the simulated average plate surface velocity for an acrylic panel that is 0.457 m × 0.356 m × 3 mm thick. Mechanical metrics for acrylic are $E = 3.2 \times 10^9$ Pa, $\nu = 0.37$, and $\rho = 1180\ \frac{\text{kg}}{\text{m}^3}$. The shapes taken by the exciters in the simulations are a point source, disc with $r = 25.4$ mm and a thin ring with $r_O = r_I = 25.4$ mm placed at location (0.170 m, 0.132 m). For all three exciter shapes, the magnet mass is 30 g and the spring constant is $k = 14316\ \frac{\text{N}}{\text{m}}$. From Eqs. (18) and (19), the cutoff frequency of this material for a disc would be 3.29 kHz and for a thin ring would be 1.86 kHz.

To demonstrate that cutoff frequency is independent of exciter location, Fig. 7(b) shows the same types of responses as in Fig. 7(a) but with the exciter location moved to (0.366 m, 0.285 m). Comparing Figs. 7(a) and 7(b), the amplitudes

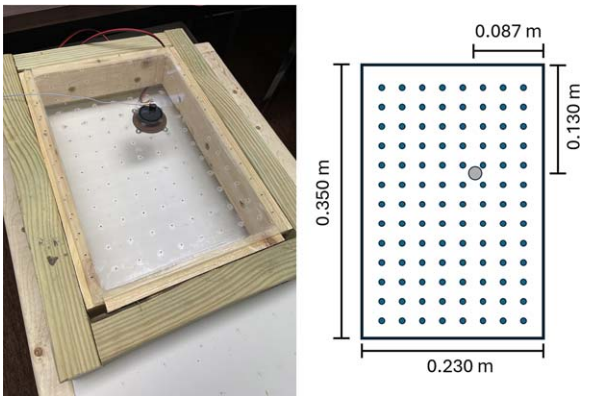

Fig. 8. The clear acrylic panel used in the experimental validation with the large disc-type exciter attached underneath and the accelerometer attached to the top. A diagram of the dimensions of the panel is also shown with the location of the exciter labeled and shown as a gray circle. Small blue circles are measurement points.

of the peaks and troughs have slightly changed, but the nodes due to the disc and ring stay the same.

Additionally, Fig. 7(c) shows the same types of responses but for a plate with smaller dimensions of 0.229 m × 0.178 m and the exciter placed at (0.084 m, 0.066 m), illustrating that the panel dimensions and the disc/ring effects are also mostly independent.

2.2 Acoustic Response

Fig. 7(d) shows the acoustic sound pressure level response that was simulated using the Rayleigh integral. The mean value (plotted) is determined by averaging the responses at 37 positions located on a semicircle 1 m from the center of the plate. The plate is assumed to be completely baffled and in an anechoic environment. The effects of the disc and ring exciter shapes can be seen on the acoustic output at high frequencies, similar to the velocity behavior.

3 EXPERIMENTAL VALIDATION

To test and validate the equations derived in this paper, a 3-mm-thick acrylic panel with dimensions 0.350 m × 0.230 m was constructed. This plate is caulked at the edges to thick wooden supports, approximating near-fixed boundary conditions. The excitation location is chosen as a constant (0.130 m, 0.087 m) for all excitation source shapes. The plate acceleration is measured using a chirp test signal with a PCB Piezotronics 352A24 accelerometer connected to a 480C02 preamplifier, placed at plate locations spaced 1 inch apart, for a total of 112 measurement locations. The experimental setup with the large disc-shaped exciter attached is shown in Fig. 8. Panel velocity measurements as shown in Fig. 9 are then calculated as the average acceleration over all measurement points divided by frequency to match the simulation output.

The first exciter chosen is the Dayton Audio DAEX32EP-4, due to its wide ring that couples it to the plate. The exciter weighs 0.136 kg and has a spring constant of roughly $k = 15000\ \frac{N}{m}$ with a ring where $r_O = 21$ mm and $r_I = 10.5$ mm. Experimental results are given in Fig. 9(a) and show a close match between simulation and experiment, although the simulation-predicted first node is slightly lower in frequency than the experimental results. This effect is likely due to the fact that the actual exciter's ring is rigidly connected to the voice coil with a cylinder that has a radius of 16 mm, and the actual wider ring that attaches to the plate is likely flexible enough that it does not apply force evenly.

Although this experiment has confirmed that the ring coupling shape causes a node in the frequency response, a topic for future work is to look for patterns in the errors

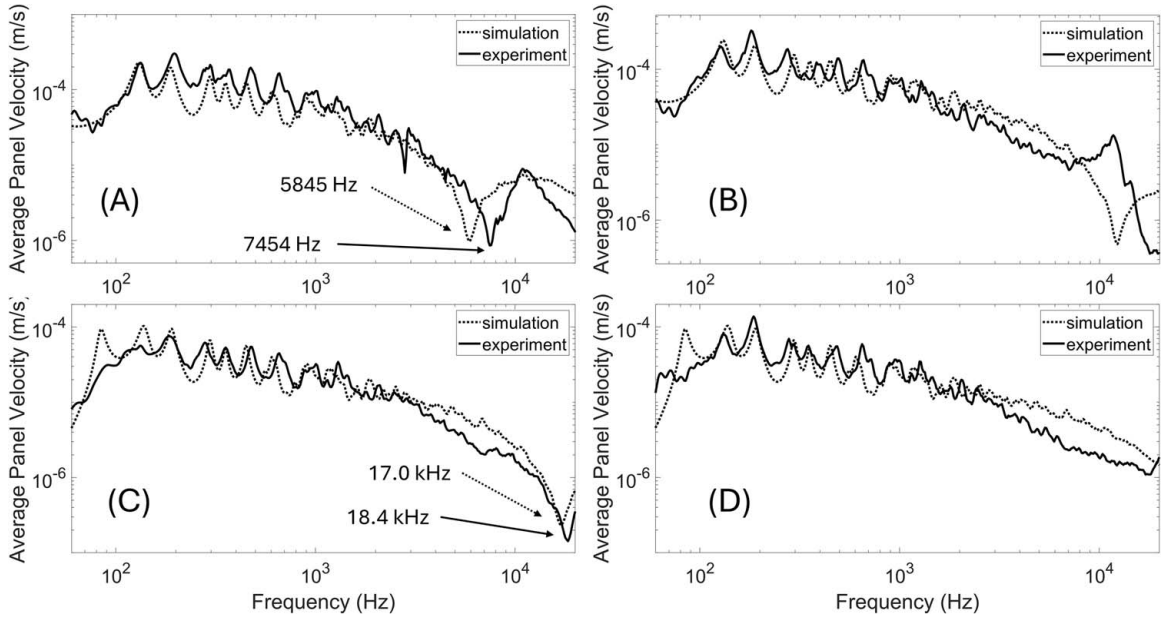

Fig. 9. Graphs of simulated vs. experimentally measured plate surface velocity in response to (a) a large ring-type exciter, (b) a large disc-type exciter, (c) a small ring-type exciter, and (d) the small ring-type exciter from (c) but with a 3D-printed disc attachment.

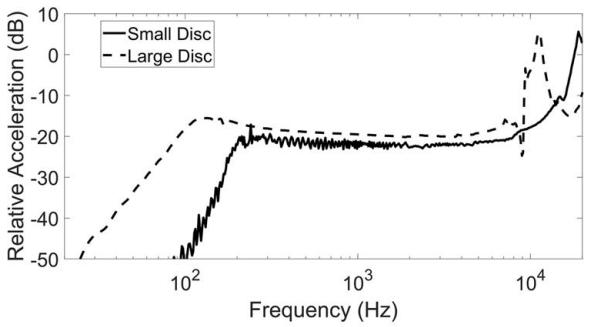

Fig. 10. The experimentally measured acceleration profiles of the large disc-type exciter used in the experiment of Fig. 9(b) demonstrating a resonance around 11 kHz and the small disc-type exciter used in Fig. 9(d), demonstrating a resonance near 20 kHz.

between the nodal frequencies predicted by the equations in this paper and experimental data. The errors may be normally distributed around the predicted nodal frequency, indicating that manufacturing tolerances play a large role in the cutoff frequency or systematically offset, indicating that a correction factor needs to be included that likely models the flexibility of the ring.

The second exciter, the Dayton Audio EX25FHE2-4 IMS, was chosen because its coupling surface is a disc rather than a ring. This exciter has a mass of 113 g, a spring constant of roughly $k = 14000\ \frac{N}{m}$, and a disc radius $r = 16$ mm. The velocity responses of the plate to this exciter are shown in Fig. 9(b), where the measured results show good agreement at low frequencies (where C is large) but less agreement at high frequencies. This is because, as seen in Fig. 10, the disc-type exciter exhibits its own resonance (equivalent to cone breakup in a traditional loudspeaker) at roughly 11 kHz that alters the frequency response of the plate.

Finally, a third exciter was selected to determine whether it was possible to turn the lower-cutoff ring behavior into higher-cutoff disc behavior. Because the disc must be fairly rigid to avoid breakup resonances and a smaller exciter radius makes this easier, a smaller unit was chosen: the Dayton Audio DAEX19CT-4. This exciter has a mass of 0.023 kg and a spring constant of roughly $k = 14000\ \frac{N}{m}$. The ring has $r_O = 10.5$ mm and $r_I = 8$ mm. A graph of simulation vs. experiment for the ring setup is shown in Fig. 9(c), again indicating close agreement between the simulation and experiment.

To turn the ring into a disc shape, a 3D-printed cylinder with $r = 10.5$ mm and a height of 4 mm was created and super glued to the exciter's ring. Anything thinner than this would likely not have had enough stiffness to act like a true disc at high frequencies and provide force evenly. The experimentally measured acceleration for this exciter with the 3D-printed disc coupler is shown in Fig. 10, indicating that the smaller disc still has a breakup resonance near 20 kHz. Results for this setup are shown in Fig. 9(d), demonstrating that the ring node was almost entirely removed, although it does appear that there may be a noticeable resonance effect near the highest end of the measured spectrum.

The small 3D-printed disc does indeed have a resonance here, as measured and illustrated in Fig. 10. This experiment demonstrates that discs do indeed have higher cutoff frequencies than rings, as the model would predict, but it turns out to be very difficult to fabricate a ring that behaves as the model would predict at high frequencies due to the disc itself having breakup resonances.

4 CONCLUSION

In this paper, a mathematical model was derived for understanding how the disc or ring shape of a voice coil exciter for flat-panel loudspeakers will affect the frequency response. It was found that the effects are dependent on the material properties of the plate that the exciter is attached to, such as thickness and Young's modulus, and are actually independent of the plate dimensions. Rings have a notch in the response at a lower frequency than discs, but discs attenuate higher frequencies more rapidly overall than rings.

It was also found, experimentally, that rings are well simulated using the equations derived in this paper. The cutoff frequency for discs is also accurate, but high-frequency results for discs do not appear to be particularly well simulated because the disc will exhibit internal breakup resonances that alter the plate response. The cutoff frequency determined in the paper can still be used for a disc to determine the frequency limit of predictable behavior. A 3D-printed small disc was also able to transform a ring structure to a disc-type coupler and extend the effective bandwidth of the exciter, confirming that a disc of the same outer radius as a ring will have a higher cutoff frequency. Looking forward, it is likely worth investigating additional shapes of exciters and methods of simulating discs that include their breakup resonances.

5 REFERENCES

[1] N. Harris and M. J. Hawksford, "The Distributed-Mode Loudspeaker (DML) as a Broad-Band Acoustic Radiator," presented at the *103rd Convention of the Audio Engineering Society* (1997 Sep.), paper 4526.

[2] K. Li, *A Critical Review of Bending Wave Loudspeaker Technology and Implementation*, M.A. thesis, Chalmers University of Technology, Göteborg, Sweden (2010 Sep.).

[3] M. C. Heilemann, D. A. Anderson, S. Roessner, and M. F. Bocko, "The Evolution and Design of Flat-Panel Loudspeakers for Audio Reproduction," *J. Audio Eng. Soc.*, vol. 69, no. 1/2, pp. 27–39 (2021 Feb.). https//doi.org/10.17743/jaes.2020.0057.

[4] V. Ganju, "Smartphone Screens Are About To Become Speakers," *IEEE Spectr.*, vol. 61, no. 3, pp. 22–27, (2024 Mar.). https://doi.org/10.1109/MSPEC.2024.10458088.

[5] M. Roberts, "Exciter Design for Distributed Mode Loudspeakers," presented at the *104th Convention of the Audio Engineering Society* (1998 May), paper 4743.

[6] D. Anderson, M. Heilemann, and M. Bocko, "Flat-Panel Loudspeaker Simulation Model with Electromagnetic Inertial Exciters and Enclosures," *J. Audio Eng. Soc.*, vol. 65, no. 9, pp. 722–732 (2017 Sep.). https://doi.org/10.17743/jaes.2017.0027.

[7] Express Parts, "Exciters and Tactile Transducers 101: An Introduction," https://www.parts-express.com/resources-buyers-guide-exciters (accessed Nov. 27, 2024).

[8] G. B. Warburton, "The Vibration of Rectangular Plates," in *Proc. Inst. Mech. Eng.*, vol. 168, no. 1, pp. 371–384 (1954 Jun.). https://doi.org/10.1243/PIME_PROC_1954_168_040_02.

[9] D. A. Anderson, Driver-Array Based Flat-Panel Loudspeakers: Theoretical Background and Design Guidelines, Ph.D. thesis, University of Rochester, Rochester, New York (2017 Mar.).

[10] L. Cremer, M. Heckl, and B. Petersson, "*Structure-Borne Sound*," (Springer-Verlag, Berlin, Germany, 2005), 3rd ed. https://doi.org/10.1007/b137728.

THE AUTHORS

David A. Anderson

David A. Anderson is an assistant professor of electrical engineering at the University of Minnesota Duluth, which he joined in 2022. He received his B.S. in electrical and computer engineering (ECE) from Colorado State University in 2012 and his M.S. and Ph.D. in 2014 and 2017, respectively, from the University of Rochester. From 2018 to 2020, he was an assistant teaching professor in ECE at the University of Pittsburgh. From 2020 to 2022 he was a senior research scientist at Applied Research Associates, Inc., and an adjunct professor at the University of Colorado Denver and University of Denver. His research interests include acoustics, vibration control, applied machine learning, and biometric sensing.